4-2022

SARS-CoV-2 Main Protease Inhibitors Repurposed for HIV-1 Protease Binding

Jacob Minkkinen
College of Saint Benedict/Saint John's University, jminkkine001@csbsju.edu

SARS-CoV-2 Main Protease Inhibitors Repurposed for HIV-1 Protease Binding

Jacob Minkkinen

The College of Saint Benedict and Saint John's University

COLG 398: Distinguished Thesis

Academic Year 2021-2022

Approved By:

Dr. Lisa Gentile

Thesis Advisor

Professor of Chemistry

Dr. Edward McIntee

Faculty Reader

Professor of Chemistry

Dr. Manuel Campos

Faculty Reader

Professor of Biology

Dr. Jen Schaefer

Faculty Reader

Professor of Biology

Dr. Alicia Peterson

Chemistry department Chair

Abstract

Severe acute respiratory syndrome (SARS-CoV-2) led to the COVID-19 global pandemic, with over 460 million cases of infection and over 6 million deaths since the start of the pandemic. SARS-CoV-2 is a retrovirus that utilizes a main protease (M^{pro}). M^{pro} is a catalytic cys/his protease. Several treatments were proposed to stop the pandemic including repurposing drugs to inhibit the M^{pro}. Another retrovirus that uses a protease is human immunodeficiency virus (HIV-1) which has been a global epidemic for 40 years and is a devastating disease that attacks the immune system. HIV-1 has infected 79.5 million people and has killed an estimated 36 million people since the start of the epidemic in 1981 and is still prevalent today. HIV-1 retrovirus utilizes the host cell's machinery to transcribe viral RNA and translate gag-pol protein. HIV-1 protease is a dual asp protease used to cleave this gag-pol protein, thereby activating the protein, allowing for viral replication and infection of other cells. HIV-1 pr can sporadically mutate into drug resistant strains which resist the common therapies used to inhibit HIV-1 pr. An approach to combat this issue is to create treatments made specifically for these drug resistant strains. In one strain, multidrug resistance is caused in the multidrug resistant hexamutant of HIV-1 pr (HIV-1 pr MDR-HM) with six amino acid mutations: (L10I/M46I/I54V/V82A/I84V/L90M). The focus of this research is to investigate whether SARS-CoV-2 M^{pro} and HIV-1 pr have a similar enough mechanism that SARS-CoV-2 M^{pro} inhibitors will also bind to both HIV-1 protease wild type (wt) and MDR-HM. Three repurposed SARS-CoV-2 inhibitors: carmofur, leupeptin, and rosuvastatin were chosen to see if they could be repurposed for HIV-1 protease due to their affordability and computational binding affinity to HIV-1 pr. Initially, computational analysis was utilized to acquire binding information of the repurposed SARS-CoV-2 inhibitors on HIV-1 protease. POCASA (Pocket Cavity Search Algorithm) was used to predict the main binding pockets of HIV-1 protease. Swissdock identified the center of the HIV-1 protease homodimer being the most prevalent binding pocket. Analysis of this pocket showed thermodynamically favorable binding to leupeptin, carmofur, and rosuvastatin. Since computational analysis showed promising prevalence for the inhibitors, the next step was to test these *in vitro*. A plasmid containing HIV-1 protease was transformed into E. coli BL21(DE3) cells. HIV-1 protease was purified from E. Coli cells and used in a fluorescent binding assay to derive binding affinity of rosuvastatin to HIV-1 pr wt (K_d=32.3 ± 3.5 μM) and MDR-HM (K_d=73.7 ± 15.8 μM), as well as carmofur to HIV-1 pr wt (K_d= 0.35 ± 0.01 mM) and MDR-HM (K_d=0.31 ± 0.04 mM).

Introduction

Background

In 2019, a severe acute respiratory syndrome coronavirus (SARS-CoV-2) belonging to the genus *betacoronavirus* led to the COVID-19 global pandemic. Since then, there has been over 460 million documented cases and over 6 million deaths[1]. On January 30th, 2020, the Director-General of the World Health Organization (WHO) declared that the outbreak of coronavirus a Public Health Emergency of International Concern (PHEIC)[2]. Many pharmaceutical treatments were repurposed to inhibit or stop the virus including inhibiting its protease. Shown in figure 2, a protease is like genetic scissors that cuts long inactive polyproteins, thereby activating them. Once active, the virus can use the resulting nonstructural proteins (NSPs) to now infect other cells. SARS-CoV-2's protease that does the majority of the "cutting" is called a main protease (M^{pro}). Inhibitors such as leupeptin, carmofur, and rosuvastatin shown in figure 6 were repurposed to fight the COVID-19 pandemic by inhibiting SARS-CoV-2's M^{pro}. Leupeptin is a naturally occurring protease inhibitor, carmofur is an anticancer drug commonly used to treat gastric and bladder cancers, and rosuvastatin is commonly used to lower LDL cholesterol and triglycerides in the blood. Given that all of these drugs have bioavailability and can be taken by humans, they make excellent candidates to repurpose.

Similarly, human immunodeficiency virus (HIV-1) has been a global epidemic for 40 years and is a devastating disease that attacks the immune system; HIV-1 has infected 79.5 million people and killed a staggering 36 million people since the start of the epidemic in 1981[3]. HIV-1 is the predecessor to acquired immunodeficiency syndrome (AIDS). AIDS eventually causes the immune system to fail, which gives rise to cancers and diseases throughout the body. Since the start of the epidemic over 32.7 million people have died from AIDS related illnesses[3]. There is no known cure for HIV-1, although there are medicines that can lessen the toll that HIV-1/AIDS takes on the body. In 2019, there were 38 million people living with HIV-1 and 1.7 million of those people being new HIV-1 infections. Reportedly, 690,000 people died of AIDS related illnesses in 2019. Comparably, this was 40% less than the peak of 1.7 million AIDS related deaths in 2004[3]. Therefore, HIV-1/AIDS is still prevalent to this day. The research question this

thesis focuses on is what effect, if any, will repurposed SARS-CoV-2 M^{pro} inhibitors have on HIV-1 protease? The goal is to observe if repurposed SARS-CoV-2 M^{pro} inhibitors will bind to HIV-1 protease; the results were evaluated both computationally and *in vitro*.

SARS-CoV-2 mechanism of action

SARS-CoV-2 is an RNA virus that exploits host cell machinery to replicate and repackage its genome to infect subsequent host cells. The mechanism of host cell infection by SARS-CoV-2 is shown in figure 1.

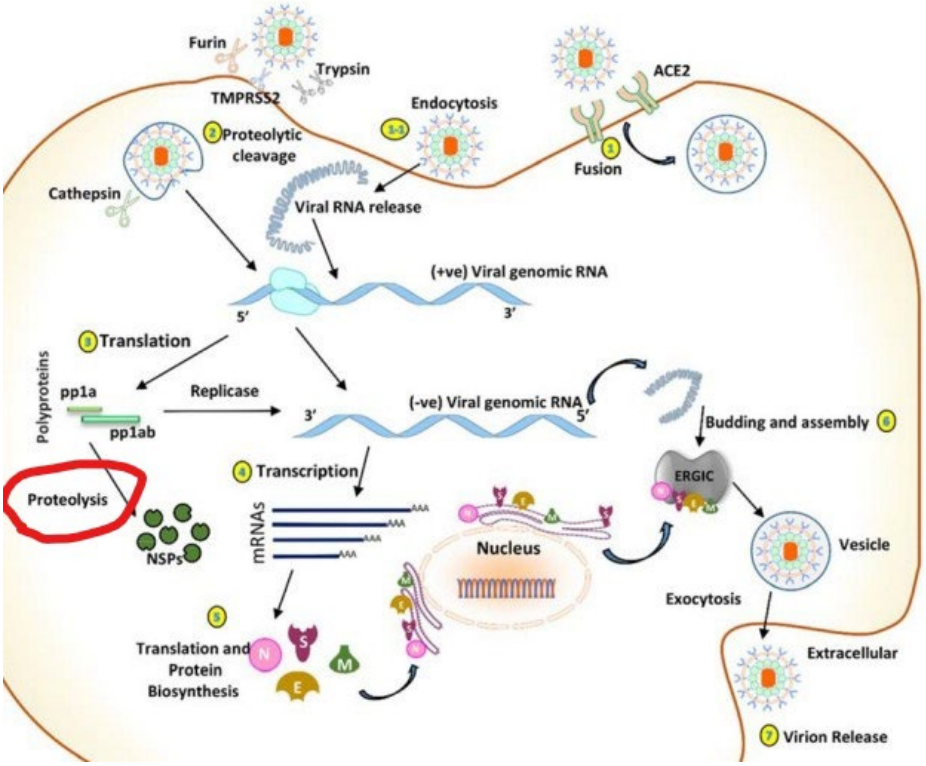

Figure 1. Mechanism of SARS-CoV-2 infection method[4].

The coronavirus genome encodes structural proteins such as the glycosylated spike (S) protein, which is needed for host cell binding and entry, and key non-structural proteins such as RNA-dependent RNA polymerase (RdRp), the main protease (M^{pro}) and papain-like protease (PL pro). These crucial proteins are translated first. During viral replication, SARS-CoV-2 M^{pro} cleaves the

viral polyproteins, to generate many NSPs needed for a functionally active viral replication complex for packaging within host cells. [5]

Figure 1 shows the SARS-CoV-2 viral particle binds to the ACE-2 receptor and enters via receptor-mediated endocytosis (1). Once inside the viral capsid is degraded by the host cell's ribosome (2). SARS-CoV-2 releases RNA into the host cell (3). The RNA is translated by the host cell's ribosome into viral replicase polyproteins pp1a and pp1ab. However, these long polyproteins are not functional, so they need to be cleaved via a protease to be activated. Circled in red, pp1a and pp1ab are cleaved by SARS-CoV-2 M^{pro} during proteolysis, releasing non-structural proteins (NSPs) which are required for viral replication and packaging. The NSPs head to the endoplasmic reticulum for folding, once folded they can enact viral replication and packaging.[6] Drugs such as carmofur, leupeptin, and rosuvastatin have been tested *in vitro* and showed inhibition to SARS-CoV-2 M^{pro}.[5]

SARS-CoV-2 M^{pro} mechanism of action

The protease that conducts the cleavage and activation of polyproteins pp1a and pp1ab in an infected cell is SARS-CoV-2 main protease (M^{pro}). This protease is imperative for viral replication, so naturally, many drugs were sought out to be repurposed to inhibit this protease in an effort to stop the COVID-19 pandemic. The functional portion of the SARS-CoV-2 M^{pro} catalytic active site contains a cysteine and a histidine; an example of this mechanism of the cys/his protease is shown in figure 2. In step one, covalent catalysis occurs where histidine deprotonates the SH on cysteine resulting in S- which is a better nucleophile. The cysteine side chain (S-) does a nucleophilic attack where the two electrons on the sulfur attack the carbon of the carbonyl backbone of the long polyprotein. In step two the histidine (on the left) protonates the amino group via donating a proton, making the amino group a good leaving group. Pi donation occurs where the electrons in the tetrahedral intermediate shift resulting in the amino group leaving, and a separate thioester complex being formed in the third step of figure 2. In step three, histidine deprotonates a water molecule to make OH- which is a better nucleophile. Thermodynamically, this thioester is favorably attacked by the deprotonated water resulting in amine (in blue) and carboxylic acid (in red) products.

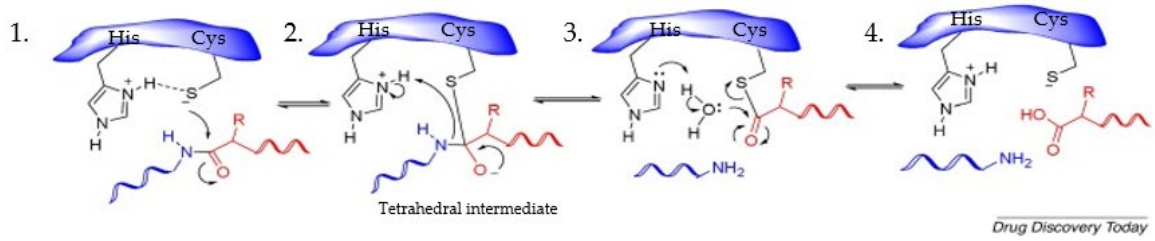

Figure 2. Mechanism of SARS-CoV-2 M^{pro} cys/his protease.[5]

The mRNA vaccines manufactured by Pfizer, Johnson and Johnson, and Moderna proved to have an immensely higher efficacy in thwarting the pandemic than SARS-CoV-2 M^{pro} inhibitors.[7] Therefore, the vaccines were the safer and easier alternative therapies for SARS-CoV-2. However, SARS-CoV-2 RNA-dependent RNA polymerase has the tendency to cause frequent mutations[8], and only has efficacy for so long before mutation of the virus. Mutations which increase severity of infection or rate of infection are causes for concern[9]. So other avenues for inhibiting SARS-CoV-2 should be considered, including SARS-CoV-2 antivirals. Repurposing antivirals for mechanistically similar viruses is a common pharmacokinetic approach.

HIV-1 mechanism of action

Similar to SARS-CoV-2, HIV-1 is also an RNA virus. Seen in figure 3, the HIV capsid contains 2 copies of single-stranded (ss) RNA as well as reverse transcriptase (RT) and integrase. The capsid is surrounded by a membranous envelope, on the envelope there are two glycoproteins (gp120 and gp41) which facilitate binding to the CD4 receptor. Upon binding, gp120 undergoes a conformational change which allows it to bind to the chemokine receptors CCR5 and CXCR4. Once this happens, gp41 reaches the surface of the host cells and ligates the virus capsid to the host cell. The conformational change at gp41 and viral capsid ligation promotes endocytosis of the viral particle into the host cell. The capsid is then destroyed by the host cell's lysosome, releasing the viral contents within the host cell[10]. After viral envelope degradation, a complimentary DNA copy is reverse transcribed from the viral RNA genome made by RT. RT then degrades the RNA strand and uses the ssDNA as a template to make double stranded (ds)

DNA; ds DNA is then spliced into the host cell DNA by the integrase enzyme. Transcription of the viral genome from the newly made dsDNA leads to the production of more viral RNA. Some of the viral ssRNA is incorporated into new virions. The rest of this is translated into gag (capsid proteins), env (gp120 and gp41), and pol (RT, integrase, and protease) pro-proteins.[11] HIV-1 protease cleaves these pro-proteins to release RT, integrase, and viral structural proteins; HIV protease is required to cleave the gag and gag-pol polyproteins into their final functional protein products, leading to the assembly of a fully mature and infectious viral particle.[12] Since the role of the protease is pertinent to HIV-1's maturation and infection, it is one of the protein targets to inhibit to reduce viral load.

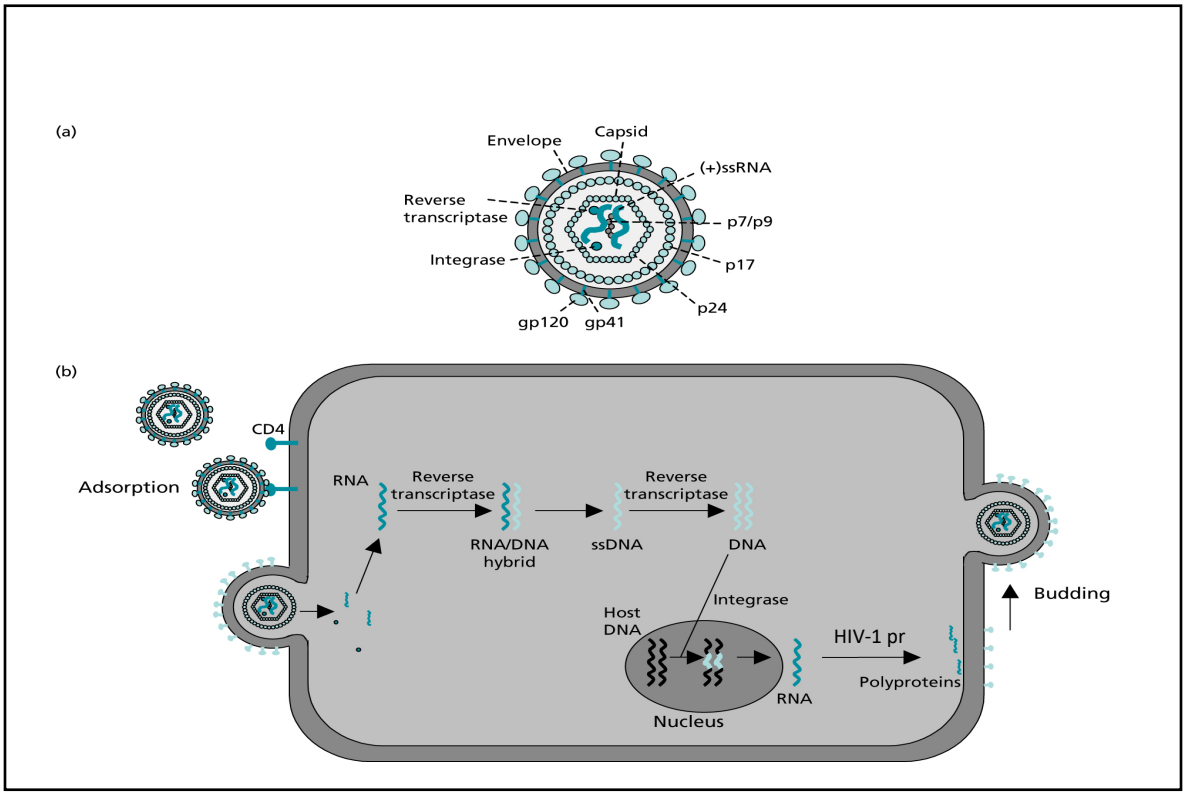

Figure 3. (a) HIV-1 viral particle and respective contents inside (b) HIV-1 viral particle infecting a host T-Cell by binding to the CD4 receptor.[11]

HIV-1 pr mechanism of action

HIV-1's protease mechanism isn't unlike SARS-CoV-2's M^{pro}. HIV-1's dual aspartyl groups are the active units of the HIV-1 homodimer. The aspartyl protease mechanism that HIV-1 protease

utilizes is shown in figure 4; in step one, an aspartic acid deprotonates a water molecule to make OH- which is a better nucleophile. The deprotonated water attacks the carbon on the carbonyl backbone of the polyprotein on the top of figure 4. In step 2, pi donation occurs where the electrons in the tetrahedral intermediate shift resulting in the leaving of the protonated amino group resulting in a carboxylic acid and amine products (cleaved polyprotein) in the third step.

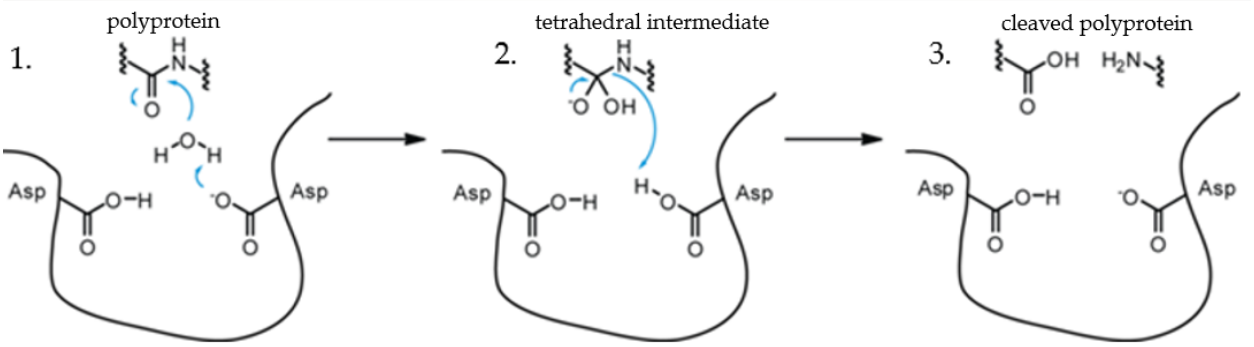

Figure 4. Mechanism of the homodimer HIV-1 protease.[13]

A continued difficulty in fighting the HIV-1 epidemic is that the virus can sometimes mutate into drug resistant strains which resist the common therapies used to inhibit HIV-1 pr. An approach to combat this issue is to create treatments made specifically for these drug resistant strains. In one strain, multidrug resistance is caused in the multidrug resistant hexamutant of HIV-1 pr (HIV-1 pr MDR-HM) because of six mutations in the protease molecule: leu 10, met 46, ile 54, val 82, ile 84, and leu 90[14]. This mutant is resistant to currently used clinical HIV-1 pr therapies such as indinavir, nelfinavir, saquinavir, ritonavir, amprenavir, and lopinavir.

This thesis tested repurposed SARS-CoV-2 inhibitors on both HIV-1 protease wild type (wt) and multidrug resistant hexamutant (MDR-HM) with 6 amino acid mutations (L10I/M46I/I54V/V82A/I84V/L90M)[14]. Although the amino acid groups on the active sites of SARS-Cov-2 M^{pro} and HIV-1 pr are different, the mechanism between the two is similar. This thesis investigated whether these two proteases have a similar enough mechanism that repurposed SARS-CoV-2 M^{pro} inhibitors will bind to HIV-1 protease.

Computational work

Computational tools used

Computational tools that were used in this study were POCASA, SwissDock, chimera, and PyMOL. POCASA (Pocket cavity search application)[15] uses the program *Roll* which uses the enzymes' known 3D structure and rolls a probe sphere along the enzyme to detect binding pockets and depth centers of the enzyme. These binding pockets show where potential small molecules, such as repurposed inhibitors, can bind. SwissDock is a molecular modeling program that provides possible molecular interactions between a ligand in various orientations, and a specific protein.[16] The results from SwissDock and POCASA can be combined and visualized by PyMOL[17] to observe the prevalence of binding of each repurposed drug. Computational binding prevalence is the number of binding orientations of a small molecule in the central binding pocket, divided by the total number of binding orientations observed. Chimera was also used in observing intermolecular forces between the repurposed SARS-CoV-2 M^{pro} inhibitors and HIV-1 pr wt and MDR-HM. Summary of this process is illustrated in figure 5, binding prevalence results are shown in figure 8, and computational binding affinities are shown in figure 9.

Computational methods

In this study, SARS-CoV-2 M^{pro} inhibitors were tested to target HIV-1 protease. The inhibitors carmofur, leupeptin, and rosuvastatin, shown in figure 6, were selected from 'Potential SARS-CoV-2 main protease inhibitors' (Banerjee, R. et al., 2020)[5]. These proposed inhibitors shown in figure 6 were selected to be repurposed because they had medicinal use already which has shown to be safe for human consumption at a low dose; carmofur's LD50 for oral administration to rats is 268 mg/kg, leupeptin's LD50 for oral administration to rats is 1.5 g/kg, and rosuvastatin's LD50 for oral administration to rats is 14.5 g/kg.[21, 22, 23] Additionally, these inhibitors were selected because they were relatively cheap and attainable to be used for *in vitro* lab research.

Figure 5. Flowchart of computational steps using SwissDock, POCASA, Chimera, and PyMOL.

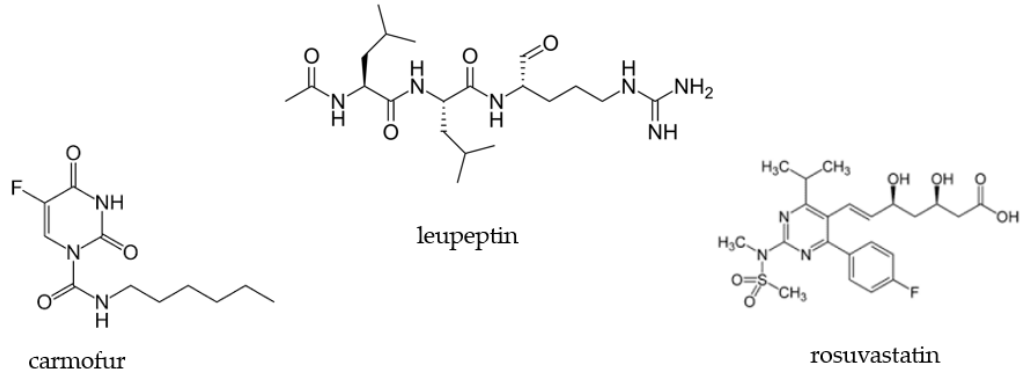

Figure 6. SARS-CoV-2 M^{pro} inhibitors chosen to be repurposed for HIV-1 pr inhibition.

POCASA was used to observe the primary binding pocket of HIV-1 protease. The SARS-CoV-2 M^{pro} inhibitors selected to be repurposed had their binding energies and orientations evaluated by SwissDock. Binding prevalence was observed; if a high quantity of inhibitor orientations bound to the HIV-1 protease pocket, the intermolecular forces (IMFs) between HIV-1 pr and the inhibitors were then observed in Chimera, if favorable IMFs and thermodynamically favorable binging energies could be observed then these inhibitors were tested *in vitro.*

Computational results

POCASA was used to determine the binding pocket of HIV-1 protease shown in figure 7. This was done for both wild type (wt) and multidrug resistant-hexamutant (MDR-HM)[14] with six amino acid mutations: (L10I/M46I/I54V/V82A/I84V/L90M). Shown on the right in figure 7, the binding pocket was determined to be in the center of the active-form homodimer and adjacent to the asp 25 active site.

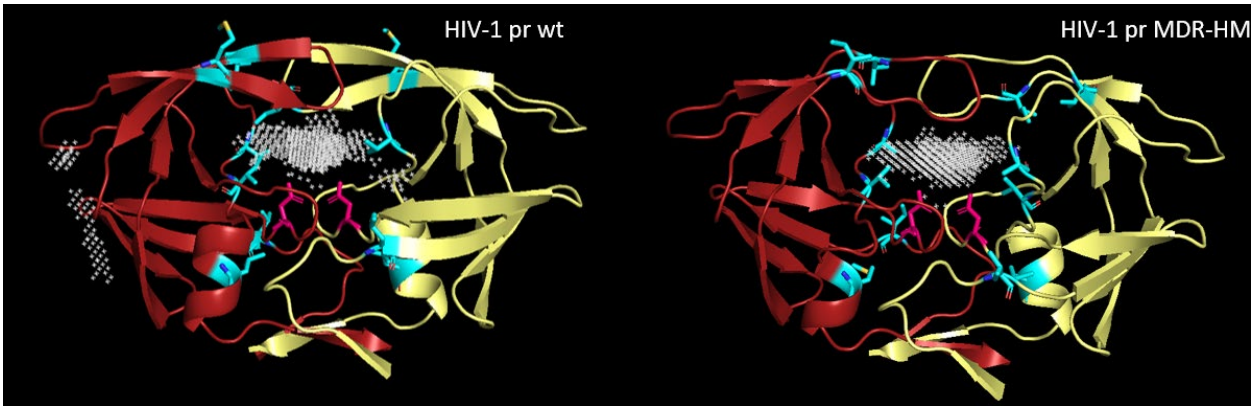

Figure 7. PyMOL image of POCASA results. Binding pockets shown as small white dots. Aspartyl protease active site is colored pink. Turquoise regions on wt represent the regions in MDR-HM which represent the mutated amino acids (L10I/M46I/I54V/V82A/I84V/L90M).

Computational binding prevalence was then evaluated, results shown in figure 8. There was high binding prevalence for both HIV-1 pr wt and MDR-HM. The computational IMFs and binding energies were observed in Chimera shown in figure 9.

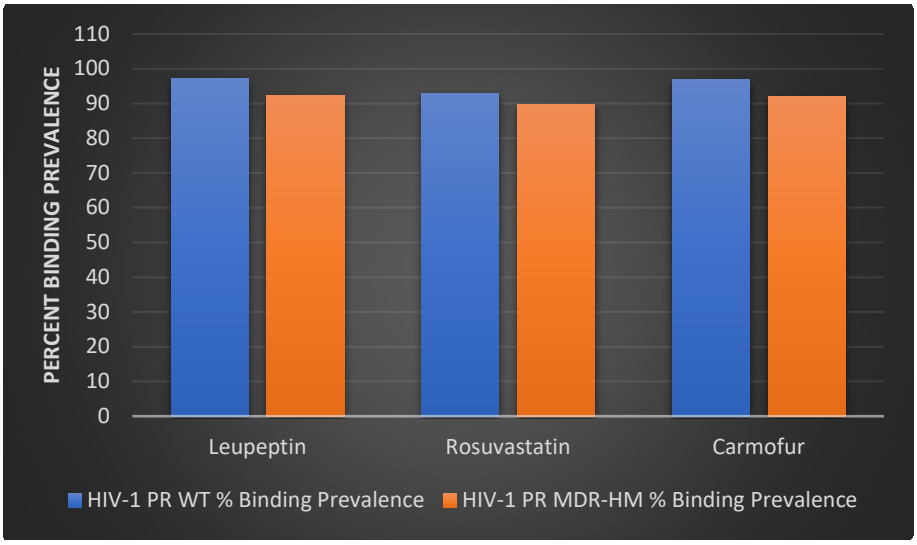

Figure 8. Comparison of overall binding prevalence of leupeptin, rosuvastatin, and carmofur; between HIV-1 pr wt and MDR-HM.

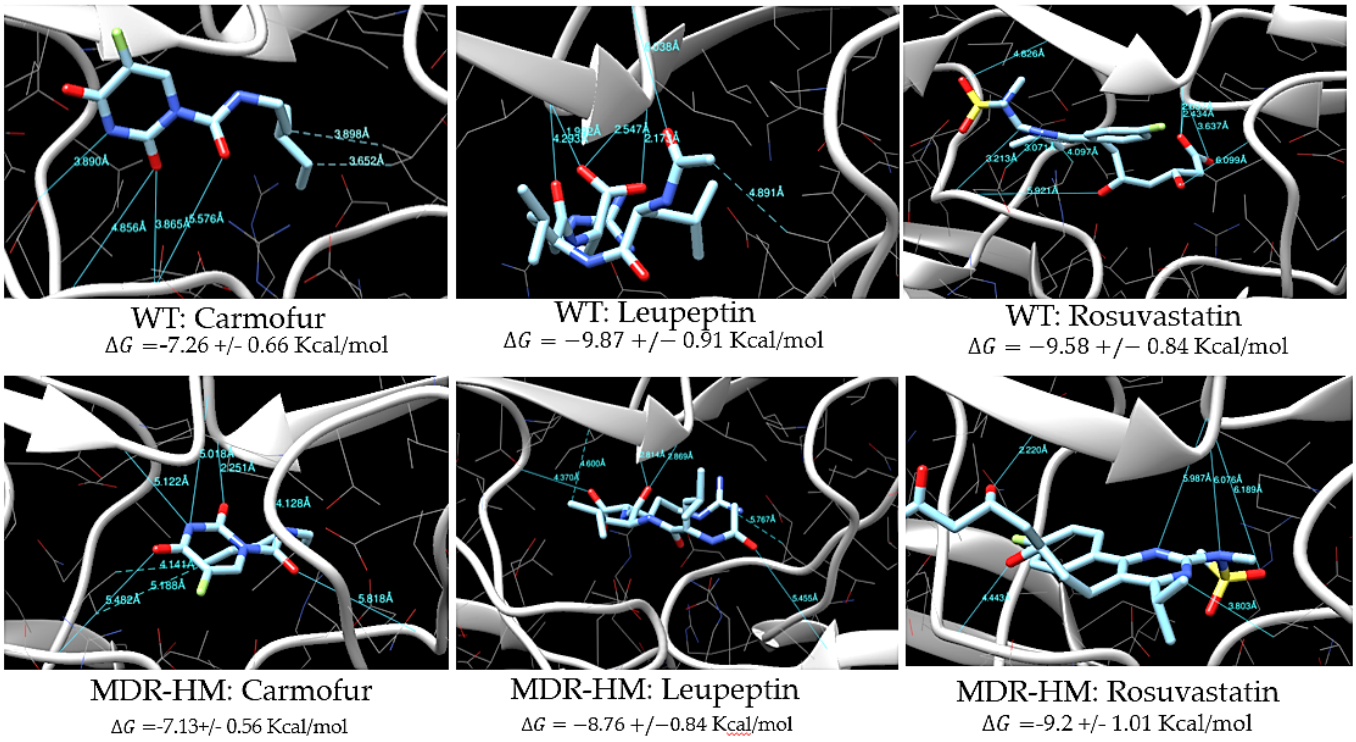

Figure 9. Close up Chimera image of carmofur, leupeptin, and rosuvastatin within the binding pocket of HIV-1 pr wt and MDR-HM. HIV-1 pr is colored silver, and potential inhibitors are in light blue. Small blue and yellow lines represent IMFs within the pocket favorably binding to each binding pocket. IMF listings are located in table 3 of supplemental materials.

Computational evidence for carmofur, leupeptin, and rosuvastatin includes having high binding prevalence to both HIV-1 pr wt and MDR-HM binding pockets and having strong binding affinities to that pocket. The next steps to be taken were to purchase the molecules and test them on a purified HIV-1 pr wt and MDR-HM *in vitro*.

In vitro Lab Methods

Expression and purification of the HIV-1 pr wt and MDR-HM

Recombinant HIV-1 pr was expressed in transformed E. coli BL21(DE3) cells containing a pET24 vector containing the coding sequence for HIV-1 pr. HIV-1 pr was purified by a modification of the procedure from Pettit. S., et al.[18] The pET24 vector that contains the gene for HIV-1 protease expression was taken up by BL21 (DE3) strain of E. coli. Transformed

BL21(DE3) E. coli were grown in Luria broth (LB) to an optical density 600nm (OD_{600}) of 0.6. 1mM IPTG was added to inhibit the repressor to induce expression, the cells were incubated at 37ºC for 3 hours. Following induction of expression, E. Coli cells were centrifuged at 5000 rpm for 20 min at 4ºC, then the supernatant was decanted. Isolated inclusion bodies were resuspended in 40 ml 50 mM Tris HCl, and 5mM dithiothreitol (DTT). The resuspended inclusion bodies were sonicated and centrifuged at 10,000 x g for 10 min. Isolated inclusion bodies were solubilized overnight in 10 ml of a buffer containing 8 M guanidine hydrochloride, 50 mM Tris-HCl (pH 7.5), and 5 mM DTT. The solubilized protein was clarified by centrifugation at 11,500 x g at 4ºC for 15 min. The HIV-1 pr in the filtrate was precipitated by the addition of 10 volumes of methanol and stirred at 4ºC for 10 minutes, which was then placed at -20°C for 1 hour. White precipitate was seen and collected by centrifugation at 25,000 x g at 4ºC for 20 min. The pellet was resuspended in 3 ml of a buffer containing 8 M urea, 20 mM Tris-HCl (pH 7.5), 2 mM dithiothreitol, and 2 mM EDTA. The concentration of protein in the 8 M urea solution was determined with a biorad assay, and the volume of the solution was adjusted to a concentration of less than 1 mg/ml. HIV-1 pr was refolded by rapid dilution into 20 volumes of ice-cold folding buffer containing 20 mM sodium acetate (pH 5.5), 1 mM EDTA, 2.5 mM dithiothreitol, and 10% glycerol. After refolding, any leftover insoluble aggregated protein was removed by centrifugation at 25,000 x g for 15 min. The resulting high-speed supernatant was dialyzed overnight in 1L folding buffer. Refolded HIV-1 pr was aliquoted and stored at -80°C. HIV-1 pr obtained by this procedure was evaluated by sodium dodecyl sulfate-polyacrylamide gel electrophoresis (SDS-PAGE). SDS-PAGE gel image is shown in figure 10. This procedure was conducted for both HIV-1 pr wt and MDR-HM.

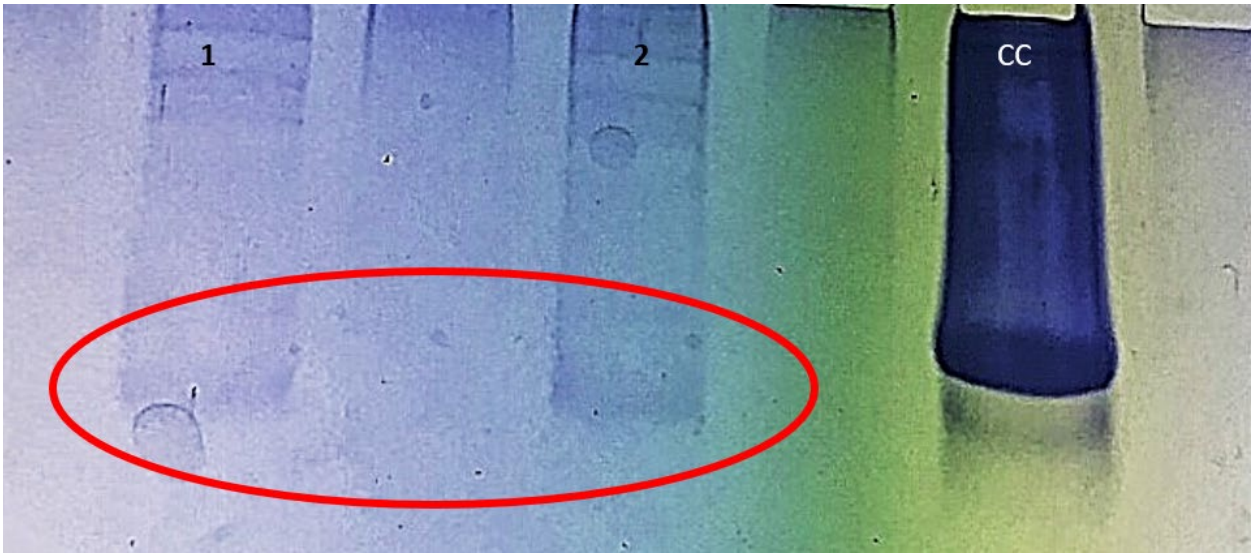

Figure 10. 15% SDS-PAGE gel. Lane labeled 1 is HIV-1 Pr wt(10.8 kDa) at 0.201 mg/ml; lane labeled 2 HIV-1 pr MDR-HM(10.8 kDa) at 0.135 mg/ml. Lane 3 is a concentrated cytochrome C MW (12kDa) marker.

Binding assays:

Proteins that contain aromatic amino acids tryptophan, tyrosine or phenylalanine can be excited by UV light in the 260-290nm region and will emit UV light at a higher wavelength. This process is called fluorescence and an example is in figure 11.

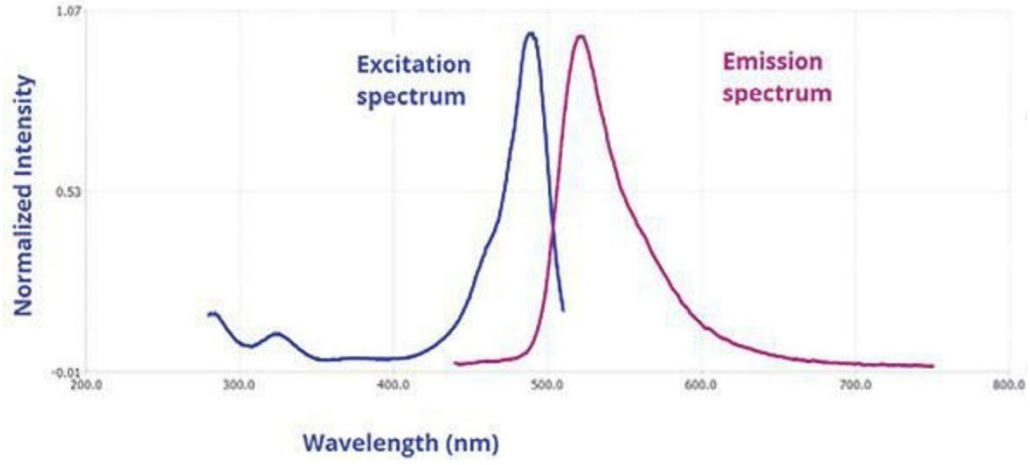

Figure 11. An example how fluorescence works, where a molecule is excited at a specific wavelength and emitting light at a longer wavelength. Figure is from Principles of Fluorescence Spectroscopy 3rd edition[19].

When an inhibitor binds to the protein, a conformational change in the protein may occur and the environment surrounding the tryptophan residues can change. This binding is observed with a change in lambda max and a change in fluorescent intensity. When the tryptophan residues are shifted into a less polar environment the λ_{max} decreases and fluorescent intensity increases. When the tryptophan residues are shifted into a more polar environment, like in this experiment, the λ_{max} increases and fluorescent intensity decreases. This process is called intrinsic fluorescence quenching. In this experiment, only the fluorescent tryptophan residue was observed, phenylalanine has a low quantum yield and tyrosine can easily be quenched and therefore isn't a viable residue to rely on for quenching.[20] This fluorescent quenching technique is used to measure the binding affinity between proteins and ligands. HIV-1 protease dimer has four tryptophan amino acids in total with two trp residues on each monomer (trp6, trp 41, trp105, trp140) that can be excited and thus emit fluorescence. Fluorescent quenching with inhibitors interacting with HIV-1 pr residues can be quantified. Therefore, fluorescent binding assays were conducted with leupeptin, carmofur, and rosuvastatin to measure the binding affinity between these inhibitors and HIV-1 pr.

Binding assay methods:

250 μL of HIV-1 pr wt (0.201 mg/ml) and MDR-HM (0.135 mg/ml) in folding buffer (20 mM sodium acetate (pH 5.5), 1 mM EDTA, 2.5 mM dithiothreitol, and 10% glycerol) was put into a 96 well plate. Increasing volumes from 0-7μL of rosuvastatin (5mg/ml), carmofur (15mg/ml), and leupeptin (16mg/ml) were used in subsequent binding assays. Rosuvastatin, carmofur, and leupeptin were all solubilized in DMSO. Rosuvastatin binding assay used enzyme: inhibitor mole to mole ratio of 1.1 to 56.5 for HIV-1 pr wt and 0.8 to 38 for HIV-1 pr MDR-HM. Carmofur binding assay used an enzyme: inhibitor mole to mole ratio of 0.2 to 10 for HIV-1 pr wt and 0.1 to 6.8 for HIV-1 pr MDR-HM. No binding was detected for leupeptin at any concentration with the fluorescent method used in this assay, the highest concentration of leupeptin used in the binding assay which used enzyme: inhibitor mole to mole ratio of 0.3 for HIV-1 pr wt, and 0.2 for HIV-1 pr MDR-HM.

Samples were measured at fluorescent excitation of 290 nm to isolate tryptophan residues, and emission was observed between 300 and 400 nm. Binding assays were done for both HIV-1 pr wt and MDR-HM. Dissociation constants (K_d) were derived from trend lines to observe the binding strength of respective inhibitors; K_d is the inverse of association constant (K_a). A low K_d means strong binding affinity; [EI] $\rightleftharpoons$ [E]+ [I] where E is the enzyme, I is the inhibitor, and EI is the enzyme-inhibitor complex. So therefore, $\frac{[E][I]}{[EI]} = K_d$. From an experimental standpoint, the equation $\frac{\mathbf{1}}{\Delta \boldsymbol{F}} = \frac{\mathbf{1}}{\boldsymbol{F_\infty - F_0 \times Kd[L]}} + \frac{\mathbf{1}}{\boldsymbol{F_\infty - F_0}}$ can be used to calculate the K_d from the resulting quenching. F_0 is the fluorescence intensity in the absence of inhibitor, F_∞ is the fluorescence intensity with saturating concentration of inhibitor, F is the fluorescence intensity at some particular [inhibitor], and ΔF is ($F - F_0$).

Binding assay results and analysis:

Increasing concentrations of respective carmofur and rosuvastatin yielded raw data shown in figure 15 in supplemental information. Fluorescent quenching for both HIV-1 pr wt and MDR-HM. Rosuvastatin (enzyme: inhibitor mole to mole ratio was 1.1 to 56.5 for HIV-1 pr wt and 0.8 to 38 for HIV-1 pr MDR-HM) was observed to have a stronger reduction of fluorescence indicating a stronger binding than carmofur (enzyme: inhibitor mole to mole ratio was 0.2 to 10 for HIV-1 pr wt and 0.1 to 6.8 for HIV-1 pr MDR-HM). Carmofur also showed fluorescent quenching indicating binding. Shown in table 1, the inhibitor to enzyme molar ratios are much higher for carmofur than rosuvastatin, but rosuvastatin consisted of a ~10^{-2} difference in K_d.

Table1. Respective K_d values and inhibitor to enzyme molar ratios.

Repurposed M^{pro} inhibitors	K_d **(HIV-1 wt)**	K_d **(HIV-1 MDR-HM)**	**enzyme: inhibitor mole ratio (wt)**	**enzyme: inhibitor mole ratio (MDR-HM)**
carmofur	0.35 ± 0.01 mM	0.31 ± 0.04 mM	0.2 to 10.0	0.1 to 6.8
rosuvastatin	32.3 ± 3.5 μM	73.7 ± 15.8 μM	1.1 to 56.5	0.8 to 38.1

Figure 12 shows raw data of the highest concentration of leupeptin used in the binding assay which used enzyme: inhibitor mole to mole ratio of 0.3 for HIV-1 pr wt, and 0.2 for HIV-1 pr MDR-HM. No intrinsic fluorescent quenching was detected, therefore, no conformational change occurred which put trp into a different environment.

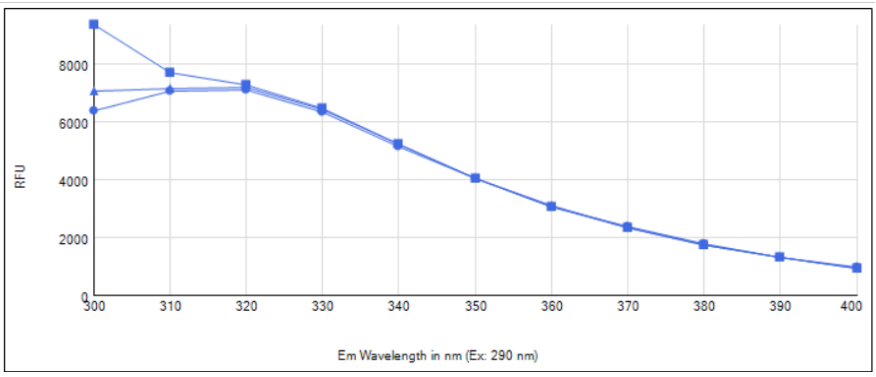

Figure 12. Fluorescent quenching analysis of 250 µL HIV-1 Pr wt and 7 µl leupeptin (16mg/ml) triplicates, each line represents a trial.

Carmofur, and rosuvastatin were dissolved in DMSO at their respective solubilities; a control experiment was done with DMSO to verify that it didn't quench the fluorescence of HIV-1 pr on its own. The raw data results shown in figure 13 indicate DMSO did not impact the fluorescence of HIV-1 pr.

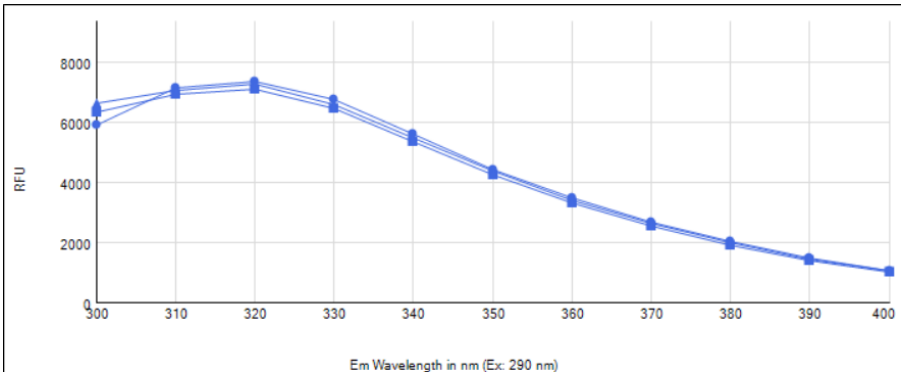

Figure 13. 250 µL HIV-1 pr wt and 7µL DMSO triplicates, each line represents a trial.

Discussion:

The raw data in figure 15 in was used to create figure 14 shown below. The K_d was derived for carmofur and rosuvastatin. Shown in figure 14, rosuvastatin and carmofur showed binding to HIV-1 pr wt and MDR-HM. Although this binding is minimal, the repurposed SARS-CoV-2 M^{pro} inhibitors rosuvastatin and carmofur did show binding to HIV-1 pr wt and MDR-HM nonetheless. Table 2 shows a comparison in binding between the repurposed SARS-CoV-2 M^{pro} inhibitors for HIV-1 pr, and currently used clinical therapies for HIV-1 pr[14].

Table 2. Respective K_d of each inhibitor on HIV-1 protease. First portion of the table consists of repurposed SARS-CoV-2 M^{pro} inhibitors on HIV-1 pr; the second portion is already used clinical therapies for HIV-1 pr.

Repurposed M^{pro} inhibitors	**Carmofur**	**Rosuvastatin**				
wt	0.35 ± 0.01 mM	32.3 ± 3.5 µM				
MDR-HM	0.31 ± 0.04 mM	73.7 ± 15.8 µM				
Clinically used therapies	**Indinavir**	**Nelfinavir**	**Saquinavir**	**Ritonavir**	**Amprenavir**	**Lopinavir**
wt	0.76 ± 0.04 nM	0.44 ± 0.04 nM	0.28 ± 0.02 nM	0.098 ± 0.008 nM	0.20 ± 0.01 nM	0.0083 ± 0.0014 nM
MDR-HM	150 ± 10 nM	93 ± 5 nM	550 ± 20 nM	150 ± 30 nM	17 ± 1 nM	5.5 ± 0.8 nM

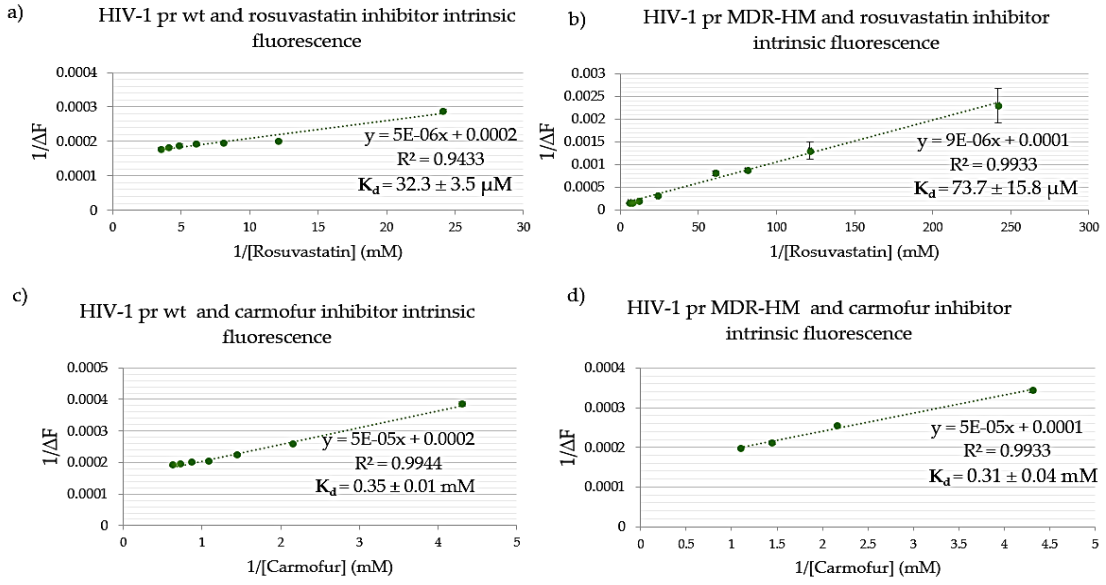

Figure 14. Graphs derived from fluorescent quenching data in figure 10; a) HIV-1 pr wt and rosuvastatin K_d=32.3 ± 3.5 µM; b) HIV-1 pr MDR-HM and rosuvastatin K_d=73.7 ± 15.8 µM; c) HIV-1 pr wt and carmofur K_d= 0.35 ± 0.01 mM; d) HIV-1 pr MDR-HM and carmofur K_d=0.31± 0.04 mM.

Conclusion and future directions

Computational work was done by utilizing POCASA to elucidate binding pockets of HIV-1 pr wt and MDR-hm. And used SwissDock to compare different orientations of carmofur, leupeptin, and rosuvastatin to derive binding prevalence to HIV-1 pr wt and MDR-HM. The computational work done in this thesis shows repurposed SARS-CoV-2 M^{pro} inhibitors having high binding prevalence to both HIV-1 pr wt and MDR-HM with favorable thermodynamic binding. This determined which inhibitors to select for binding *in vitro*.

Repurposed SARS-CoV-2 M^{pro} inhibitors carmofur and rosuvastatin were tested on HIV-1 pr wt and MDR-HM *in vitro*. Results in table 2 showed relatively weak binding affinities. When comparing rosuvastatin and carmofur K_d values to the K_d values of current clinically used inhibitors for HIV-1 pr for HIV-1 pr wt, indinavir (K_d=0.76 ± 0.04 nM), nelfinavir (K_d=0.44 ± 0.04 nM), saquinavir (K_d=0.28 ± 0.02nM), ritonavir (K_d=0.098 ± 0.008 nM), amprenavir (K_d=0.20 ± 0.01 nM), and lopinavir (K_d=0.0083 ± 0.0014nM).[14] Rosuvastatin and carmofur have minimal binding affinities (high dissociation constants) in comparison. This comparison suggests that binding isn't as efficient as currently used clinical therapies for HIV-1 pr wt and HIV-1 MDR-HM. This data suggests that the active sites for SARS-CoV-2 M^{pro} and HIV-1 pr are not similar enough for unmodified repurposed SARS-CoV-2 M^{pro} inhibitors.

The next step would be to conduct activity assays; binding assays show what has bound to HIV-1 pr but does not indicate which inhibitors have interrupted activity of the protease. Therefore, the next steps would be to conduct an activity assay of HIV-1 pr wt and MDR-HM with rosuvastatin and carmofur; because although with weak binding, there is still a possibility of these inhibitors inhibiting the dual aspartyl protease shown in figure 4.

The next steps also include doing size exclusion chromatography with the HIV-1 pr dimer. This will be done to ensure an active-form dimer has been created. If only inactive-form monomer HIV-1 pr is seen, it could be an indication as to why the binding of repurposed SARS-CoV-2 M^{pro} inhibitors to HIV-1 pr was so weak. Due to rosuvastatin possessing the most favorable binding affinity tested, if inhibition is seen, a possible future insight would be to utilize rosuvastatin as a chemical scaffold, and chemically modify it by adding functional groups to possible increase binding affinity.

Supplemental information

Table 3. Computational IMF data showing bond lengths and types of each inhibitor contained in HIV-1 pr's central pocket.

	HIV-1 pr wt			HIV-1 pr MDR-HM	
	carmofur			carmofur	
Å	**I ●●●E**	**Bond type**	**Å**	**I ●●●E**	**Bond type**
3.9	R-NH●●●O=C-O Asp 30	H-bonding	5.1	R-NH●●●O=C Gly 49	H-bonding
4.9	R-C=O●●●HN-Asp 30	H-bonding	5.0	R-NH●●●O=C Ile150	H-bonding
3.9	R-C=O●●●HN-Asp 29	H-bonding	2.3	R=O●●●HN- Ile 150	H-bonding
5.6	R-C=O●●●HN-Asp 30	H-bonding	5.8	R=O●●●HN-Asn 183	H-bonding
3.9	R-CH3●●●CH3 Val 181	London dispersion forces	5.5	R=O●●●HN-Asn 29	H-bonding
3.7	R-CH3●●●CH3 Val 182	London dispersion forces	4.1	R-CH3●●●CH3 Val 83	London dispersion forces
			5.2	R-CH3●●●CH3 Val 84	London dispersion forces
			4.1	R-CH3●●●CH3 Ile 50	London dispersion forces
	leupeptin			leupeptin	
Å	**I ●●●E**	**Bond type**	**Å**	**I ●●●E**	**Bond type**
4.3	R-C=O●●●HN-Ile50	H-bonding	4.4	R=O●●●HN- Ala 182	H-bonding
2.0	R-C=O●●●HN-Ile 50	H-bonding	2.8	R=O●●●HN- Ile 50	H-bonding
2.5	R-C=O●●●HN-Ile 149	H-bonding	2.9	R=O●●●HN- Ile 150	H-bonding
2.2	R-C=O●●●HN-Ile 149	H-bonding	5.5	R=O●●●HN-Leu 23	H-bonding
6.0	R-C=O●●●HN-Gly 151	H-bonding	4.6	R-CH3●●●CH3 Ile 50	London dispersion forces
4.9	R-CH3●●●CH3 Val 82	London dispersion forces	5.8	R-NHCH●●●CH3 Val 84	London dispersion forces
	rosuvastatin			rosuvastatin	
Å	**I ●●●E**	**Bond type**	**Å**	**I ●●●E**	**Bond type**
4.8	R-C=O●●●HN-Gly 147	H-bonding	2.2	R=O●●●HN- Gly 148	H-bonding
3.2	R=N●●●HN-Asp 129	H-bonding	4.4	R=O●●●HN- Asp 130	H-bonding
3.1	R-NH●●●O=C-O Asp 129	H-bonding	6.0	R=N●●●HN-Ile 50	H-bonding
5.9	R-C=O●●●HN-Asp 129	H-bonding	6.1	R=N●●●HN-Ile 50	H-bonding
2.0	R-C=O●●●HN-Ile 149	H-bonding	6.2	R=O●●●HN- Ile 50	H-bonding
2.4	R-C=O●●●HN-Ile 50	H-bonding	3.8	R-CH3●●●CH3 Ala 82	London dispersion forces
3.6	R-C=O●●●HN-Ile 50	H-bonding			
6.1	R-C=O●●●HN-Val 82	H-bonding			
4.1	R-CH3●●●CH3 Ile 183	London dispersion forces			

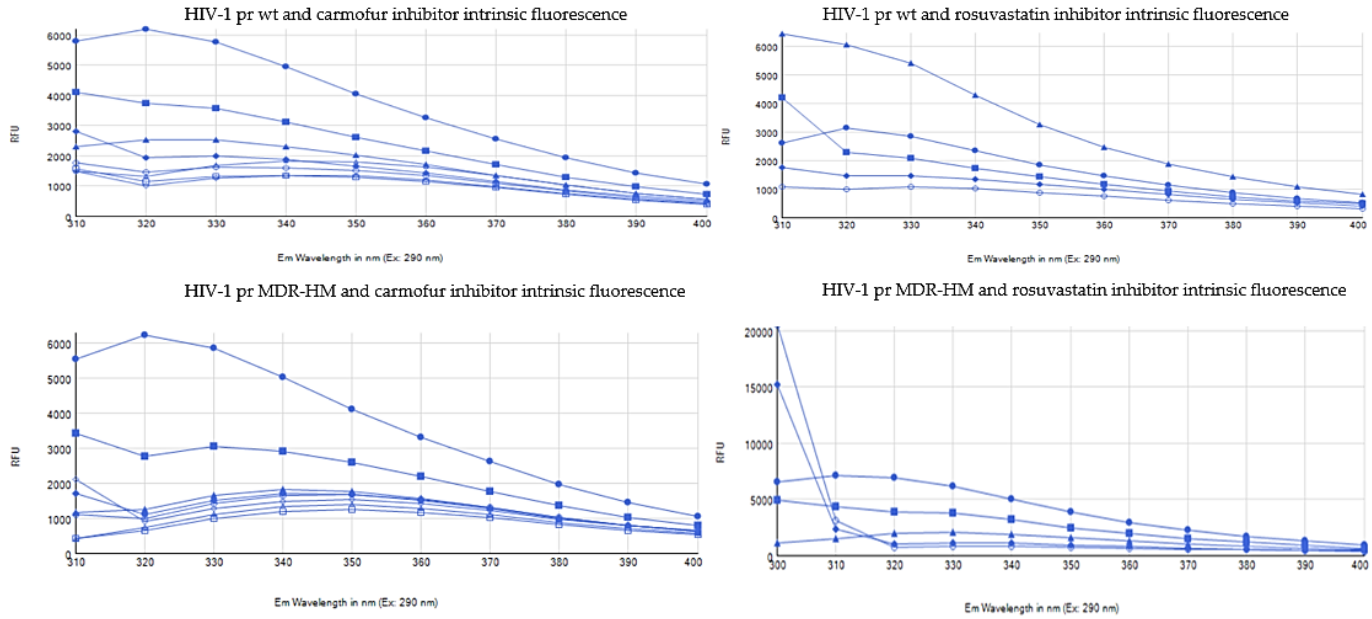

Figure 15. Raw data of fluorescent binding assay excitation of 290 nm, each line represents a trial, trials were done in triplicates; emission observed from 310 to 400 nm. This assay used carmofur (enzyme: inhibitor mole to mole ratio was 0.2 to 10 for HIV-1 pr wt and 0.1 to 6.8 for HIV-1 pr MDR-HM) and rosuvastatin (enzyme: inhibitor mole to mole ratio was 1.1 to 56.5 for HIV-1 pr wt and 0.8 to 38 for HIV-1 pr MDR-HM).

Acknowledgements

I would like to acknowledge and thank my Distinguished Thesis Committee members, and especially my advisor Dr. Gentile, for helping and mentoring me through this process. I would like to thank CSB/SJU Undergraduate Research Fund which funded my summer salary, my meeting travel, and supplies which made this research possible. I would like to thank Freiri lab for both plasmids used in this thesis. And I appreciate the entire chem department for the help and encouragement throughout my college career. I am truly grateful for all the academic experiences throughout my college career that shaped me to be the student I am today. I would like to acknowledge my family for their incessant support in my endeavors to pursue and understand science.

References

(1) **Organization, W. H.** WHO Coronavirus (COVID-19) Dashboard. 2022.
(2) Eurosurveillance Editorial, T. Note from the editors: World Health Organization declares novel coronavirus (2019-nCoV) sixth public health emergency of international concern. *Euro Surveill* **2020**, *25* (5). DOI: 10.2807/1560-7917.ES.2020.25.5.200131e From NLM.
(3) Greene, W. C. A history of AIDS: looking back to see ahead. *Eur J Immunol* **2007**, *37 Suppl 1*, S94-102. DOI: 10.1002/eji.200737441 From NLM.
(4) Yesudhas, D.; Srivastava, A.; Gromiha, M. M. COVID-19 outbreak: history, mechanism, transmission, structural studies and therapeutics. *Infection* **2021**, *49* (2), 199-213. DOI: 10.1007/s15010-020-01516-2 From NLM.
(5) Banerjee, R.; Perera, L.; Tillekeratne, L. M. V. Potential SARS-CoV-2 main protease inhibitors. *Drug Discovery Today* **2021**, *26* (1878-5832 (Electronic)), 804-816. From 2021 Mar.
(6) Santerre, M.; Arjona, S. P.; Allen, C. N.; Shcherbik, N.; Sawaya, B. E. Why do SARS-CoV-2 NSPs rush to the ER? *J Neurol* **2021**, *268* (6), 2013-2022. DOI: 10.1007/s00415-020-10197-8 From NLM.
(7) Anand, P.; Stahel, V. P. Review the safety of Covid-19 mRNA vaccines: a review. *Patient Saf Surg* **2021**, *15* (1), 20. DOI: 10.1186/s13037-021-00291-9 From NLM. Mahdi, M.; Mótyán, J. A.; Szojka, Z. I.; Golda, M.; Miczi, M.; Tőzsér, J. Analysis of the efficacy of HIV protease inhibitors against SARS-CoV-2's main protease. *Virol J* **2020**, *17* (1), 190. DOI: 10.1186/s12985-020-01457-0 From NLM.
(8) Duffy, S. Why are RNA virus mutation rates so damn high? *PLoS Biol* **2018**, *16* (8), e3000003. DOI: 10.1371/journal.pbio.3000003 From NLM.
(9) Otto, S. P.; Day, T.; Arino, J.; Colijn, C.; Dushoff, J.; Li, M.; Mechai, S.; Van Domselaar, G.; Wu, J.; Earn, D. J. D.; et al. The origins and potential future of SARS-CoV-2 variants of concern in the evolving COVID-19 pandemic. *Curr Biol* **2021**, *31* (14), R918-r929. DOI: 10.1016/j.cub.2021.06.049 From NLM.
(10) Wilen, C. B.; Tilton, J. C.; Doms, R. W. HIV: cell binding and entry. *Cold Spring Harb Perspect Med* **2012**, *2* (8). DOI: 10.1101/cshperspect.a006866 From NLM.
(11) Patrick, G. *An Introduction to Medicinal Chemistry*; Oxford University Press, 2005.
(12) Clavel, F.; Mammano, F. Role of Gag in HIV Resistance to Protease Inhibitors. *Viruses* **2010**, *2* (7), 1411-1426. DOI: 10.3390/v2071411 From NLM.
(13) Brik, A.; Wong, C. H. HIV-1 protease: mechanism and drug discovery. *Org Biomol Chem* **2003**, *1* (1), 5-14. DOI: 10.1039/b208248a From NLM.
(14) Ohtaka, H.; Schön, A.; Freire, E. Multidrug resistance to HIV-1 protease inhibition requires cooperative coupling between distal mutations. *Biochemistry* **2003**, *42* (46), 13659-13666. DOI: 10.1021/bi0350405 From NLM.
(15) J. Yu, Y. Z., I. Tanaka, M. Yao, Roll: A new algorithm for the detection of protein pockets and cavities with a rolling probe sphere. *Bioinformatics*, **26**(1), 46-52, (2010) [PMID:

19846440]. A new algorithm for the detection of protein pockets and cavities with a rolling probe sphere. Bioinformatics, 2010; Vol. 26, pp 46-52.
(16) Grosdidier, A.; Zoete, V.; Michielin, O. SwissDock, a protein-small molecule docking web service based on EADock DSS. *Nucleic Acids Res* **2011**, *39* (Web Server issue), W270-277. DOI: 10.1093/nar/gkr366 From NLM.
(17) Seeliger, D.; de Groot, B. L. Ligand docking and binding site analysis with PyMOL and Autodock/Vina. *J Comput Aided Mol Des* **2010**, *24* (5), 417-422. DOI: 10.1007/s10822-010-9352-6 From NLM.
(18) Pettit, S. C.; Moody, M. D.; Wehbie, R. S.; Kaplan, A. H.; Nantermet, P. V.; Klein, C. A.; Swanstrom, R. The p2 domain of human immunodeficiency virus type 1 Gag regulates sequential proteolytic processing and is required to produce fully infectious virions. *J Virol* **1994**, *68* (12), 8017-8027. DOI: 10.1128/jvi.68.12.8017-8027.1994 From NLM.
(19) Lakowicz, J. R. Principles of Fluorescence Spectroscopy. 3rd ed.; Springer: Boston, MA, 2006; pp XXVI, 954.
(20) Yammine, A.; Gao, J.; Kwan, A. H. Tryptophan Fluorescence Quenching Assays for Measuring Protein-ligand Binding Affinities: Principles and a Practical Guide. *Bio Protoc* **2019**, *9* (11), e3253. DOI: 10.21769/BioProtoc.3253 From NLM.

(21) Carmofur Safety Data Sheet; CAS-No. : 61422-45-5; Sigma-Aldrich Inc; 3050 SPRUCE ST, ST. LOUIS MO 63103, UNITED STATES; 10/10/2020

(22) Leupeptin hemisulfate salt Safety Data Sheet; CAS-No. : 103476-89-7; Sigma-Aldrich Inc; 3050 SPRUCE ST, ST. LOUIS MO 63103, UNITED STATES; 4/20/2021

(23) Rosuvastatin Safety Data Sheet; CAS-No. : 287714-41-4; AK Scientific, Inc; 30023 Ahern Ave. Union City, CA 94587, United States, 2/14/2020